*Inorg. Chem.* **2007**, *46*, 5390–5397


# Structural Characterization and NMR Study of $NaNbWO_6$ and Its Proton-Exchanged Derivatives

**Alois Kuhn,[†] María T. Azcondo,[†] Ulises Amador,[†] Khalid Boulahya,[‡] Isabel Sobrados,[§] Jesús Sanz,[§] and Flaviano García-Alvarado*,[†]**

*Departamento de Química, Universidad San Pablo-CEU, 28668 Boadilla del Monte, Madrid, Spain, Departamento de Química Inorgánica, Facultad de Ciencias Químicas, Universidad Complutense, 28040 Madrid, Spain, and Instituto de Ciencia de Materiales de Madrid, CSIC, Cantoblanco, 28049 Madrid, Spain*

Received January 25, 2007

The structural characterization of $NaNbWO_6$, prepared by the ceramic route, has been performed. Electron diffraction has shown the presence of two related phases in a 1:1 ratio, whose lattice parameters correspond to those of the well-known tetragonal tungsten bronzes (TTB) and those of a monoclinically distorted phase. In addition to basic unit cells, the morphology of the two phases has been found to be similar, but they present a slight difference in the W/Nb ratio. $^1H$ and $^{23}Na$ magic-angle spinning nuclear magnetic resonance (MAS-NMR) spectra of $NaNbWO_6$ and its proton-exchanged derivatives have been interpreted on the basis of the ideal TTB structure. The average structure and the morphology remain unchanged in $Na_{1-x}H_xNbWO_6$ derivatives. $^1H$ and $^{23}Na$ MAS-NMR spectroscopies have been used to monitor changes produced during exchange processes. It has been shown that the exchange of Na ions is mainly produced, but not exclusively, at tetragonal channels. However, a large amount of Na ions at the pentagonal channels do not exchange with protons, suggesting that these ions are needed to stabilize the TTB-like structure. A tentative distribution of sodium ions in the most-exchanged oxide, deduced from NMR results, $\sim(Na_{0.46})_p(Na_{0.08})_sH_{0.46}NbWO_6$, has been proposed. NMR spectra of $Na_{1-x}H_xNbWO_6$ indicate that two different OH groups are formed upon exchanging. The study of samples hydrated with $D_2O$ allowed us to conclude that deuterons of adsorbed water exchange with protons of the two OH groups. The proton–deuteron exchange is slow at room temperature but is strongly enhanced at 90 °C. This observation relates to the proton conductivity displayed by exchanged products under a humid atmosphere.

## Introduction

It has been previously reported that tetragonal tungsten bronzes (TTB hereafter) are able to undergo a rich soft chemistry. The simplest bronzes, $M_xWO_3$, have been extensively studied[1−4] and their structures are well-known.[4] Octahedra [$WO_6$] share corners to form a 3D framework with tunnels of different sections (triangular, square, and pentagonal in a 2:1:2 ratio) running along the *z* direction (Figure 1, inset). Some of the tunnels can be occupied by alkali metal, ions, or molecules.[1,2] However, different compositions of $Na_xWO_3$ can be accommodated in this structure by changing the partial occupancy of the tunnels.[4] For $x = 0.6$, all of the pentagonal and square section channels are completely filled ($Na_6W_{10}O_{30}$ when referring to the unit cell), and as $x$ decreases, sodium vacancies are created. At $x = 0.4$, that is, $Na_4W_{10}O_{30}$, all of the pentagonal channels are occupied, but channels with the square section are empty. For $x < 0.4$, sodium vacancies are also created in pentagonal channels.

At the beginning of the 21st century, there is a demand for protonic conductors at low temperature for fuel-cell electrolytes. TTB $M_xWO_3$ bronzes are characterized by nonstoichiometry in inserted, intercalated, or exchanged element ($Na^+$ or $H^+$ for instance) and by a transition element

* To whom correspondence should be addressed. E-mail: flaga@ceu.es.
† Universidad San Pablo-CEU.
‡ Universidad Complutense.
§ Instituto de Ciencia de Materiales de Madrid.

(1) Figlarz, M. *Prog. Solid State Chem.* **1989**, *19*, 1.
(2) Michel, C.; Groult, D.; Deschanvres, A.; Raveau, B. *J. Inorg. Nucl. Chem.* **1975**, *37*, 251.
(3) Horlin, T.; Marinder, B. O.; Nygren, M. *Rev. Chim. Miner.* **1982**, *19*, 231.
(4) Takusagawa, F.; Jacobson, R. A. *J. Solid State Chem.* **1976**, *18*, 163.



10.1021/ic0701312 CCC: $37.00 
Published on Web 06/01/2007

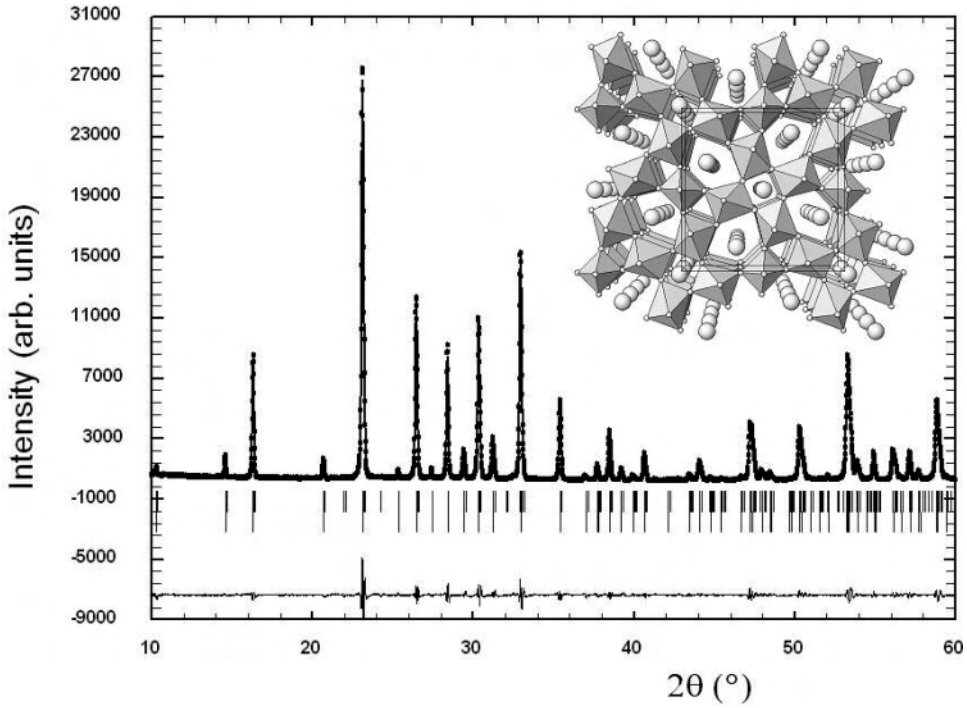


**Figure 1.** Experimental (points) and calculated (solid line) X-ray diffraction pattern (selected range) of the parent sample with nominal composition $NaNbWO_6$. The upper row of vertical bars indicates the positions of the Bragg peaks of the monoclinic phase; the peaks corresponding to the tetragonal phase are indicated by the lower row. The inset shows the schematic view of the TTB structure along the *c*-axis.

with mixed valence. Therefore, electronic conductivity is often found for such bronzes, and, hence, they could not be used as electrolytes even though ionic conductivity was high. An alternative approach for the obtention of innovative ionic conductors with no electronic contribution would be the use of oxides with a TTB-like structure, where the oxidation state of the transition metal could remain constant when the alkaline or proton content is changed. This is the case of the $Na_xNb_xW_{1-x}O_3$ series.

However, the existence range of such oxides is not clear. Previous studies of the system $NaNbO_3-WO_3$ reported the replacement of 45% W by Nb.[5] It has been pointed out that the composition with $x = 0.5$, usually formulated as $NaNbWO_6$, does not stabilize the TTB bronze but, rather, a mixture of phases. In particular, this composition was reported to produce a complicated X-ray diffraction pattern in which the presence of $WO_3$ was detected.[6,7] However, Marinder[8] reported the existence of the TTB $Na_{1.2}Nb_{1.2}W_{0.8}O_6$ phase. Finally, a TTB $NaNbWO_6$ phase was also obtained from the metastable pyrochlore $NaNbWO_6$, following a soft route.[2]

Our interest in the development of new protonic conductors drove us deep into the synthesis and characterization of both $NaNbWO_6$ and $Na_{1.2}Nb_{1.2}W_{0.8}O_6$ and the preparation of proton-exchanged derivatives. In a recent work, we reported both the synthesis of $NaNbWO_6$ by the ceramic procedure and the formation of proton derivatives.[9] The parent material was preliminarily characterized by X-ray powder diffraction as a TTB-like oxide without any evidence for $WO_3$ formation. $NaNbWO_6$ was treated with an aqueous $HNO_3$ solution to replace sodium ions with protons, producing the series $Na_{1-x}H_xNbWO_6 \cdot nH_2O$ ($0 \leq x \leq 0.46$). The electrical properties of these products were investigated. High proton-conductivity values were measured at 90 °C under a water-saturated atmosphere. Nevertheless, some doubts remained regarding the charge-carrier nature and the role of sodium ions in exchanged derivatives. In particular, because $NaNbWO_6$ was found to have a high conductivity ($10^{-3}$ S $cm^{-1}$ at 90 °C), though no protons should be present. The occurrence of spontaneous hydrolysis was pointed out as the origin of the unexpected high conductivity in the parent material.[9]

In this work, we aim for a more-detailed characterization of the parent $NaNbWO_6$ and the exchanged derivatives $Na_{1-x}H_xNbWO_6 \cdot nH_2O$ ($0 \leq x \leq 0.46$). X-ray diffraction (XRD), high-resolution electron microscopy (HREM), selected area electron diffraction (SAED), scanning electron microscopy (SEM), thermal analysis (TA), and $^1H$ and $^{23}Na$ magic-angle spinning nuclear magnetic resonance (MAS-NMR) techniques have been used to analyze structural details of the parent $NaNbWO_6$ phase. However, the characterization of exchanged products is more difficult because of the instability of the hydrated or the protonated oxides under the high-energy beam of electrons in a high-vacuum environment. In this case, samples were mainly analyzed by $^1H$ and $^{23}Na$ MAS-NMR spectroscopies to investigate the exchange process, the nature of charge carriers, and the reactivity with water.

(5) Bouillaud, Y.; Bonnin, F. *Bull. Soc. Miner. Crist.* **1965**, *87*, 700.
(6) Blasse, G. G.; dePauw, A. D. M. *J. Inorg. Nucl. Chem.* **1970**, *32*, 3960.
(7) Thakre, O. B.; Chincholkar, V. S. *Curr. Sci. India* **1972**, *41*, 735.
(8) Marinder, B. O. *Chem. Scr.* **1986**, *26*, 547.
(9) Kuhn, A.; García-Alvarado, F.; Bashir, H.; Dos, Santos, A. L.; Acosta, J. L. *J. Solid State Chem.* **2004**, *177*, 2366.

## Experimental Section

$NaNbWO_6$ and exchanged $Na_{1-x}H_xNbWO_6$ derivatives were prepared following the method reported previously.[9] For the present study, three compositions were selected: the parent $NaNbWO_6$ and the exchanged products $Na_{0.68}H_{0.32}NbWO_6 \cdot 0.1H_2O$ and $Na_{0.54}H_{0.46}NbWO_6$. These samples were previously characterized regarding their composition and thermal behavior.[9]

X-ray diffraction (XRD) patterns were recorded in a Bruker D8 high-resolution X-ray powder diffractometer, equipped with a position sensitive detector (PSD) MBraun PSD-50M, using the monochromatic Cu K$\alpha$ ($\lambda = 1.5406$ Å) radiation obtained with a germanium primary monochromator. Diffraction patterns were measured over the angular range 10−90° ($2\theta$). Step size and counting times were selected to optimize the experimental resolution. Structural features were refined by means of the Rietveld method using the Fullprof program.[10] Only the XRD data of the parent compound could be analyzed because those of the exchanged samples displayed broad complex peaks.

Structural characterization of the parent was complemented by SAED and HREM under a JEOL 3000 FEG electron microscope, fitted with a double-tilting goniometer stage (±22°). Local composition was analyzed with an INCA (Oxford) analyzer system attached to the microscope. Simulated HREM images were calculated with the multislice method using the MacTempas software package.

The morphology of microcrystals was studied by means of scanning electron microscopy (SEM), using a JEOL-JSM-5600 scanning microscope. The apparatus is equipped with an Oxford Link detector to perform energy-dispersive spectrometry (EDS) analysis.

NMR experiments were carried out in an AVANCE 400 (Bruker) spectrometer. $^1$H ($I = {}^1/_2$) and $^{23}$Na ($I = {}^3/_2$) MAS-NMR spectra were recorded at 400.13 and 105.3 MHz in presence of the external magnetic field $B_0 = 9.4$ T. Samples were spun at 4 and 10 kHz around an axis inclined at 54°44′ with respect to the magnetic field (magic-angle spinning technique). MAS-NMR spectra were recorded after irradiation of the sample with a radiofrequency pulse (single-pulse technique). $^1$H MAS-NMR spectra were recorded with a $\pi/2$ pulse (4 $\mu$s), but $^{23}$Na MAS-NMR spectra were recorded with different pulse lengths to achieve nonselective irradiation of nuclear transitions. In the last case, the pulse length was progressively reduced to obtain spectra without variations in the intensity of different components. The number of scans was 100 and 400 for the proton and sodium signals, respectively. To avoid saturation effects, the time between succesive experiments was chosen as 5s for proton and 10s for sodium signals.

NMR spectra deconvolution was carried out with the Winfit (Bruker) software package. Intensity, position, and line width of the components were determined with a nonlinear least-square iterative program. From $^{23}$Na MAS-NMR spectra, quadrupolar constants, $C_Q$, and $\eta$ were deduced from spinning side band patterns with a trial and error procedure. In this case, experimental profiles were simulated considering second-order quadrupolar interactions. In this analysis, the relative intensity and chemical shift of the components were deduced after considering the quadrupolar corrections.

## Results and Discussion

**The Parent $NaNbWO_6$.** The application of the filling scheme described by Takusagawa and Jacobson[4] to the TTB-like $NaNbWO_6$ indicates that 100% of pentagonal tunnels and 50% of square tunnels are occupied by Na ions. Because the ratio of the pentagonal to the square channel is 2:1, a random cation distribution should give a formula near to $(Na_{0.8})_p(Na_{0.2})_sNbWO_6$, where subscripts p and s refer to pentagonal and square channels.

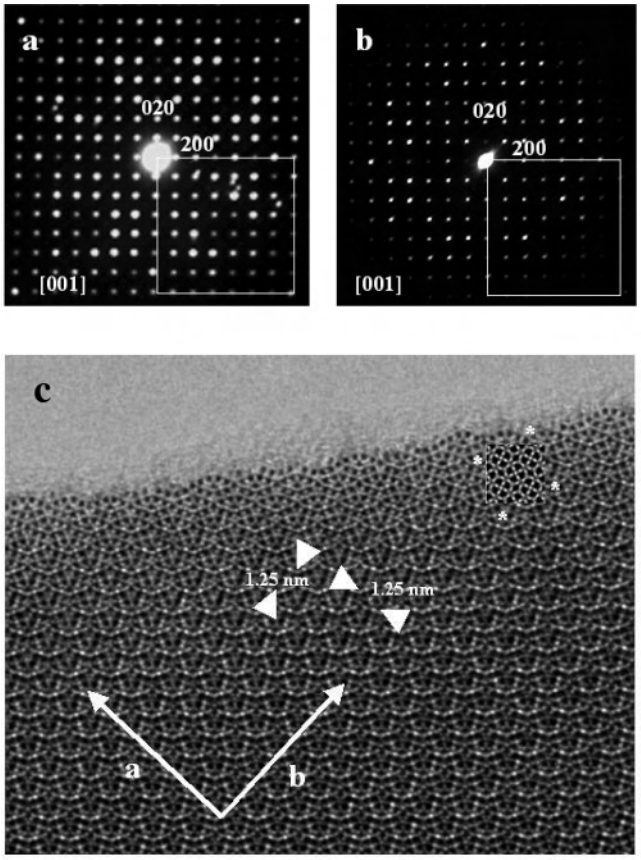


**Figure 2.** SAED patterns of the parent $NaNbWO_6$ sample: (a) crystal type 1 (MTB-like), (b) crystal type 2 (TTB-like) along [001], and (c) HRTEM image of MTB-like (crystal type 1) along [001]; a calculated image (using the ideal TTB structure, see text) is shown as an inset for Dt = 3 nm and Df = −35 nm. The lines are guides for the eye.

The X-ray powder diffraction profile of the parent $NaNbWO_6$ sample is shown in Figure 1. This pattern looks very much those of TTB-like compounds.[1−3] However, when profile matching was attempted with the tetragonal TTB model, it was evident that another related phase was present. SAED and TEM helped us to characterize the second phase.

SAED patterns revealed that two kinds of crystals coexist in the parent $NaNbWO_6$ sample. On the basis of a statistical analysis, a relative abundance of ca. 50% was estimated for each phase. Parts a and b of Figure 2 show typical SAED patterns of both types of crystals along the [001] direction. The first type of crystals present a pattern slightly distorted from the tetragonal symmetry (stressed in Figure 2a), leading to a monoclinic unit cell with a ≅ 12.5 Å, b ≅ 12.5 Å, c ≅ 3.9 Å, and $\gamma \cong 90.5°$. Because no systematic absent reflections were observed, the space group with the highest symmetry, *P*2/*m*, was assumed for this phase. The second type of crystals present the ideal TTB symmetry with parameters a ≅ 12.5 Å and c ≅ 3.9 Å (space group, *P*4/*mbm*) (Figure 2b).

(10) Rodriguez-Carvajal, J. *Physica B* **1993**, *19*, 55.

To understand the origin of such differences, we performed a detailed compositional study by energy-dispersive spectrometry (EDS) on the same crystals studied by SAED. The analysis of a representative number of crystals suggests the existence of a slight compositional difference between both phases: the TTB-like phase presents a W/Nb ratio very close to 1, whereas the monoclinic distorted phase displays a slight tungsten deficiency (W/Nb = 0.89(3)). In both phases, the sodium content has been found to be close to unity, though EDS is not sensitive enough to undoubtedly determine the sodium content. In fact, for the monoclinic phase, the obtained W/Nb ratio is not compatible with a content of one Na per formula but with a slight excess of Na (nondetectable by EDS) that may correspond to ca. $Na_{1.06}Nb_{1.06}W_{0.94}O_6$. The excess of Na is possible just by filling square tunnels slightly beyond 50% as it has been found for the so-called F phase $Na_{1.2}Nb_{1.2}W_{0.8}O_6$.

Although the Rietveld analysis of XRD data of the two phases was attempted, the complexity of both bronze-like structures (yielding a too large number of structural parameters) and the limited number of peaks in the diffraction patterns precluded a reliable structural analysis. Thus, Figure 1 presents the result of the two-phase profile matching (without structural models). The final parameters of both phases are: $a = 12.1340(3)$ Å; $c = 3.8463(1)$ Å; space group, *P*4/*mbm* for the tetragonal phase and $a = 12.1334(3)$ Å; $b = 12.0845(3)$ Å; $c = 3.8474(1)$ Å; $\gamma = 90.22(1)°$; space group, *P*2/*m* for the monoclinically distorted phase (hereafter referred to as MTB).

To shed some light on the origin of the monoclinic distortion, the two kinds of crystals were studied by HRTEM and SEM techniques. In Figure 2c, a typical HRTEM image of a monoclinic crystal taken along the [001] direction is depicted. All of the checked crystals show TTB features with d spacings of about 12.5 Å for $d_{100}$ and $d_{010}$ planes. The Fourier transformation was performed on the HREM micrographs, looking for the existence of different domains as evidence for the presence of structural distortions. Unfortunately, neither extensive defects nor W and Nb ordering or local Na ordering were detected. The contrasts observed in these images correspond to those of the ideal TTB structure. Therefore, subtle distortions detected, related probably to slight compositional differences, seem to be responsible for the monoclinic symmetry observed in half of the crystals. We performed image simulations using both structural models (TTB and MTB structures); both of them fit nicely with the experimental images. Indeed, the image calculation shown in Figure 2c (top right), corresponding to a monoclinic crystal, was performed using the ideal TTB structure.

Figure 3 shows an SEM image of the surface of a pellet of nominal composition $NaNbWO_6$. It displays a homogeneous contrast, morphology (rectangular prisms), and a narrow distribution of particle sizes. These results indicate that the two phases TTB and MTB are not distinguishable using SEM.

The $^{23}Na$ MAS-NMR spectra of the parent $NaNbWO_6$, depicted in Figure 4a, shows the presence of three different signals at $-2/-3.5$, $-8$, and $-22/30$ ppm. The two broad

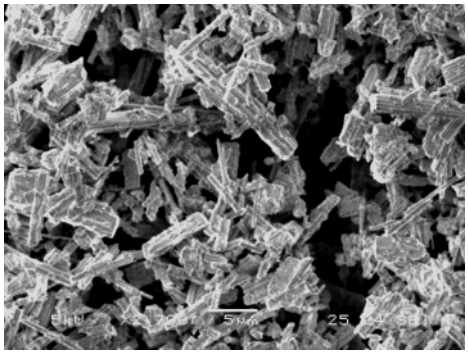

**Figure 3.** SEM micrograph of the parent $NaNbWO_6$.

signals, at $-8$ and $-22/-30$ ppm have been ascribed, in agreement with the ideal TTB structure, to sodium ions in two different crystallographic environments. The third narrow signal ($-2/-3.5$ ppm) has been attributed to mobile $Na^+_{(aq)}$ ions adsorbed at the surface of this compound. The existence of hydrated $Na^+$ ions at the surface of particles can be justified, taking into account the reactivity of the parent sample with water:

$$NaNbWO_6(s) + {}^{x}/_{2}H_2O(l) \rightarrow Na_{1-x}H_xNbWO_6(s) + (1-x)NaOH(aq)$$

This reaction was previously described by A. Kuhn et al.,[9] one of the results being that OH groups can be created by hydrolysis of the parent compound.

The irradiation of samples with radiofrequency pulses of different lengths (Figure 4a , spectra (i) and (ii)) shows that the maximum intensity of $-2/-3.5$, $-8$, and $-22/-30$ ppm signals is achieved for different times. To explain this fact, it is now accepted that strong quadrupolar interactions increase the intensity of the radiofrequency fields seen by nuclei, reducing the time required to attain the $\pi/2$ condition.[11] Taking into account that shorter times are required to achieve the maximum of the $-22/-30$ ppm band, this signal has been ascribed to Na ions located at the distorted sites of pentagonal channels. However, the signal at $-8$ ppm has been tentatively ascribed to Na ions at the regular sites of square channels. In quantitative analyses, the pulse length used in $^{23}Na$ MAS-NMR spectra recording was finally reduced to 2 $\mu$s (Figure 4a).

The analysis of quadrupolar interactions confirms this assignement (Figure 5). The simulation of the experimental profile with the Winfit program (first-order quadrupolar effects) showed that the spinning side band patterns of the $-8$ ppm component can be fitted by assuming $C_Q \cong 400$ kHz and $\eta \cong 0.5$. The analysis of the spinning side band patterns of the $-20/-30$ ppm component was more difficult, as a consequence of the broadening and the peak overlapping. The analysis of the central and satellite transitions of the $-20/-30$ ppm component (line width and asymmetry of spinning side bands) indicates that $C_Q$ must be near 1.4 MHz. In this case, the presence of intense quadrupolar interactions cause lateral transitions to shift with respect to the central

(11) Fukushima E.; Roeder, S. B. W. *Experimental Pulse NMR;* Addison Wesley, Reading, MA, 1981.

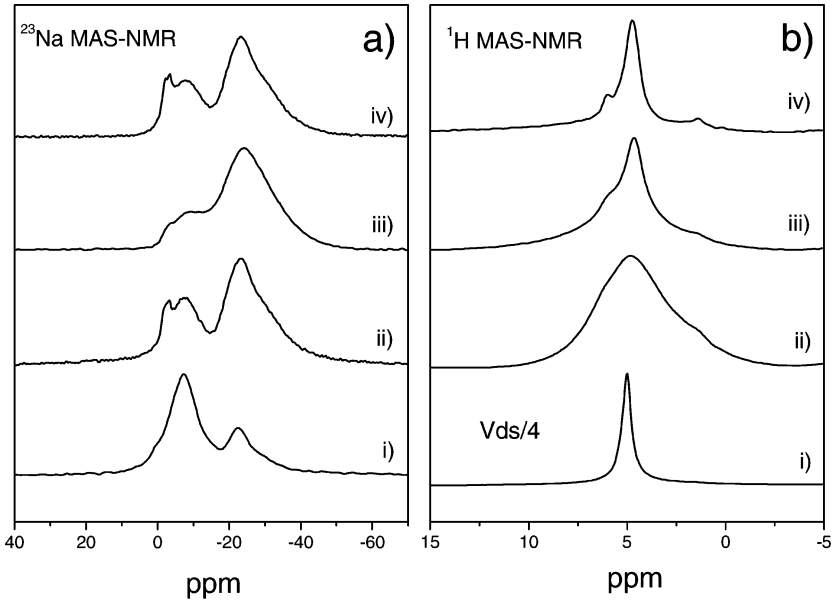


**Figure 4.** (a) $^{23}$Na MAS-NMR spectra of the parent sample $NaNbWO_6$ (i) hydrated, recorded with a 6 $\mu$s pulse, (ii) hydrated, recorded with a 2 $\mu$s pulse, (iii) dried at 60 °C, and (iv) rehydrated 20 h with $D_2O$. (b) $^{1}$H MAS-NMR spectra of the parent sample $NaNbWO_6$ (i) hydrated, (ii) dried at 60 °C, (iii) rehydrated 2 h 30 min, and (iv) rehydrated 20 h with $D_2O$.

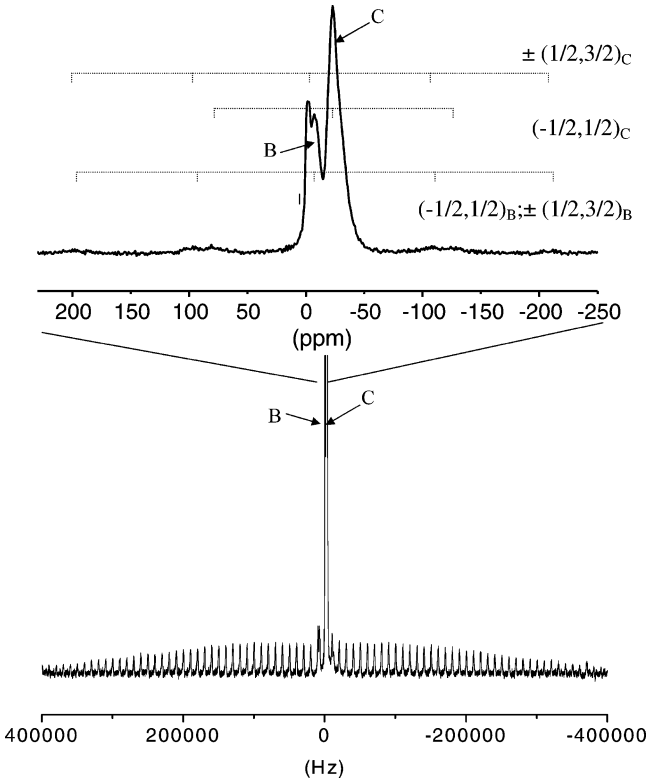


**Figure 5.** $^{23}$Na MAS-NMR spectra of the hydrated parent sample $NaNbWO_6$ illustrating the analysis of quadrupolar interactions. Satellite transitions depicted in the bottom part correspond mainly to the Na located at the square channels. Satellite transitions of Na located at pentagonal channels are not well-resolved because of its low intensity and peak overlapping.

ones. Chemical-shift values of components were deduced after the correction of second-order quadrupolar effects (−6.5 and −18/−26 ppm).

When the sample is dried at 60 °C, the broad component at −8 ppm, previously assigned to $Na^+$ located at square channels, decreases appreciably (Figure 4a, spectrum (iii)), suggesting that Na located at pentagonal channels (−22/−30 ppm component) also contributes to the −8 ppm component in hydrated samples. On the basis of this fact, it has been admitted that part of Na is coordinated to water in pentagonal channels of the $NaNbWO_6$ phase. Because the coordination of Na ions becomes more regular when they are hydrated, they give rise to a signal at chemical-shift values close to those of Na ions in square section channels. A similar argument could be applied to the −2/−3.5 ppm signal. Hydration of the $NaNbWO_6$ sample (spectrum not shown) reproduces spectral features of the starting sample. In particular, hydrated Na ions at pentagonal channels (−22/−30 ppm) shift their position to −8 ppm. The reversibility observed confirms the assignment of the band at −8 ppm to nonhydratable Na ions at tetragonal channels or to hydratable Na at pentagonal channels.

The quantitative analysis of $^{23}$Na MAS-NMR spectra was carried out on the central ($^1/_2$, $-^1/_2$) transition, by substracting the contributions of spinning side bands of lateral ($\pm^3/_2$, $\pm^1/_2$) transitions from the central one.[12] Intensities of two components, determined in samples dried at 60 °C, agree with multiplicity and occupancy of channels deduced from Takusagawa and Jacobson's model.[4] Experimental values deduced for the two components are 19 and 81%, which are very close to those calculated with this model, 20 and 80%, respectively. In TTB bronzes, the amount of pentagonal channels is double that of the tetragonal ones (Figure 1 inset), and the sodium occupancy is 100% for the former and 50% for the latter, giving finally an atomic ratio of 4:1 per formula unit. According to this fact, the structural formula $Na_5Nb_5W_5O_{30}$ can be expressed as $(Na_{0.8})_p(Na_{0.2})_sNbWO_6$, where subscripts p and s refer to pentagonal and square channels.

The $^{1}$H MAS-NMR spectrum of the $NaNbWO_6$ sample displays a single narrow component at 5 ppm that corre-

(12) Taulelle, F.; Bessada, C.; Massiot, D. *J. Chem. Phys.* **1992**, *89*, 379.

sponds to adsorbed water (Figure 4b, spectrum (i)). Once the sample was heated at 60 °C, this signal was eliminated and two small broad components at ca. 2 and 6.5 ppm, ascribed to two different OH groups, were detected (Figure 4b, spectrum (ii)). In this sample, the presence of hydrogenated species arises from the spontaneous hydrolysis of the $NaNbWO_6$ compound with atmospheric water.[9] $^1$H NMR spectra recorded after exposure of the dried sample to deuterated water (Figure 4b, spectra (iii) and (iv)) are formed again by an intense and narrow component at 5 ppm, ascribed to adsorbed water, and two additional components at 2 and 6.5 ppm, ascribed to OH groups. In these spectra, signals of two OH groups are better resolved as a consequence of the partial hydration and the partial substitution of OH by OD (OH dilution). Magnetic moments of deuterons are 6 times lower than those of protons, which considerably reduce dipolar H−H interactions that enlarge $^1$H NMR components.

All of the NMR results have been discussed on the basis of the TTB structure, and the unexpected finding regarding the presence of the MTB-related phase does not affect the above interpretation. This indicates that with NMR technique, environments of sodium and protons in both phases are similar. The presence of asymmetric bands and, even more, the presence of a shoulder in the −22/−30 band observed in $^{23}$Na MAS-NMR spectra (Figure 4a) could be taken as evidence for Na ions in more distorted sites of the monoclinic phase. However, elimination of this shoulder in H-exchanged samples does not support this assignment.

**H-Exchanged Samples.** When $NaNbWO_6$ reacts with dilute nitric acid (5 mole $dm^{-3}$), $Na^+$ ions are exchanged with $H^+$ ions according to the reaction:

$$NaNbWO_6(s) + xHNO_3(aq) \rightarrow Na_{1-x}H_xNbWO_6 \cdot nH_2O(s) + xNaNO_3(aq)$$

The maximum amount of sodium exchanged is ca. 50% after 17 consecutive treatments. This sample, $Na_{0.54}H_{0.46}NbWO_6$, is one of the samples selected for the present study. The presence of such an amount of Na ions in exchanged samples can be considered as evidence of the stabilizing role of Na ions in the TTB-like structures. However, an interesting relationship was found between the exchange rate and the presence of hydration water.[9] When the content of protons, *x*, increases, the amount of hydration water decreases, and when *x* is higher than 0.4, samples are not hydrated.

X-ray powder diffraction patterns of exchanged samples are similar to that of the parent sample $NaNbWO_6$. However, the line width of diffraction peaks becomes considerably higher. Both observations indicate that the host structure is maintained, but crystallinity decreases considerably after the topotactic exchange reaction.

The morphology and cationic content of exchanged samples have been analyzed by SEM, confirming that the exchange reaction has taken place. Figure 6 shows a representative image of a pellet of $Na_{0.54}H_{0.46}NbWO_6$, which was previously characterized by chemical and thermal analysis. In this sample, approximately half of the nominal

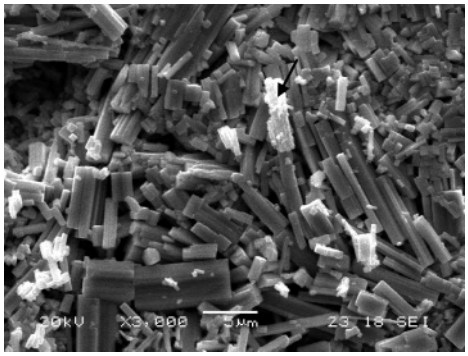


**Figure 6.** SEM micrograph of the proton-exchanged sample $Na_{0.54}H_{0.46}NbWO_6$.

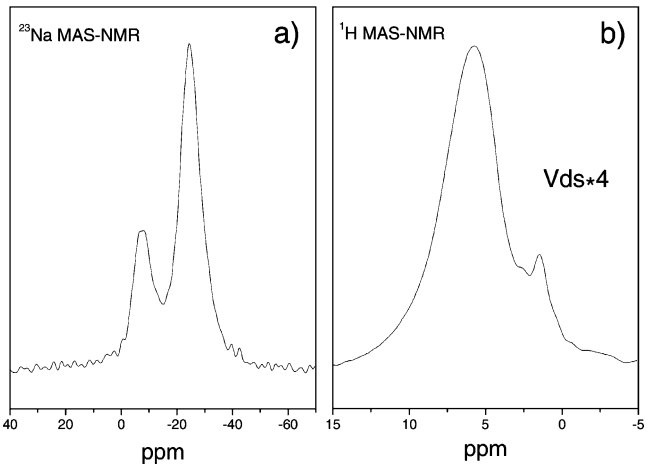


**Figure 7.** (a) $^{23}$Na and (b) $^1$H MAS-NMR spectra of the proton-exchanged sample $Na_{0.54}H_{0.46}NbWO_6$ (hydrated and dried samples display the same spectra).

Na was exchanged by protons during acid treatments. When SEM images of the parent and the exchanged derivative are compared (Figures 3 and 6), some differences are detected. In the parent sample, a rather homogeneous contrast was observed; however, in exchanged samples, particles with different contrast are observed. The majority of crystallites exhibit a dark contrast and their average cationic content deduced by EDS is near $Na_{0.60(5)}Nb_{1.0(1)}W_{1.0(1)}O_6$. However, crystallites with the white contrast are less abundant and present a higher dispersion of compositions around a mean value of $Na_{0.80(2)}Nb_{1.0(1)}W_{1.0(1)}O_6$, suggesting that the exchange reaction has not been completely achieved in all of the crystallites. Very scarce remnants of the parent $NaNbWO_6$ are also present (i.e., the crystal signaled with an arrow in Figure 6).

The $^{23}$Na MAS-NMR spectrum of the proton-exchanged sample $Na_{0.54}H_{0.46}NbWO_6$ is given in Figure 7a. The deconvolution of these spectra provided quadrupolar constants similar to those deduced for the two components in the parent sample (Figure 4a). No differences were detected in the NMR spectra after exposure of the sample to a humid atmosphere. This in agreement with the TGA analysis that showed that hydration does not take place in this sample. The comparative analysis of the $^{23}$Na MAS-NMR spectra of the parent and the H-exchanged sample (Figures 4a and 7a) shows that acid treatments produce the elimination of the narrow signal at −2/−3.5 ppm, ascribed to surface $Na^+_{(aq)}$ ions. In this sample,

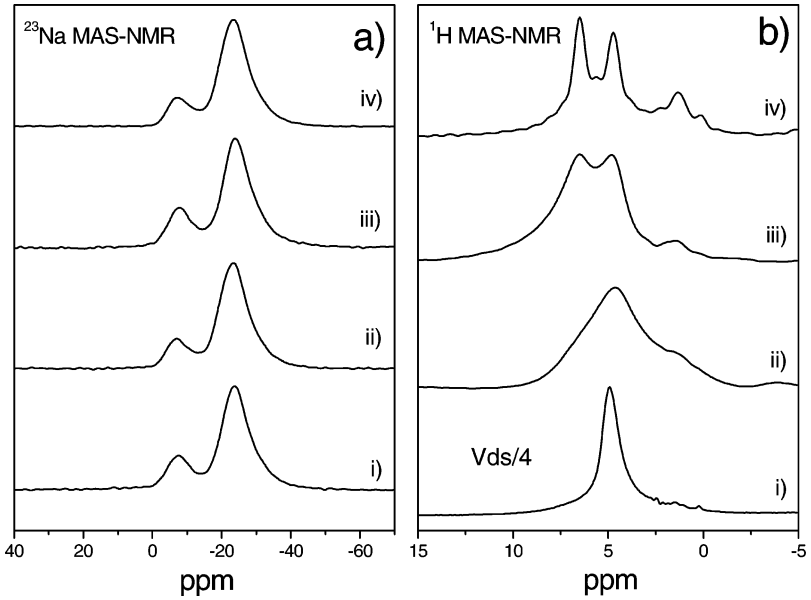


**Figure 8.** (a) $^{23}$Na MAS-NMR spectra of $Na_{0.68}H_{0.32}NbWO_6 \cdot 0.1H_2O$ (i) hydrated, recorded with a 6 $\mu$s pulse, (ii) hydrated, recorded with a 2 $\mu$s pulse, (iii) dried at 60 °C, and (iv) rehydrated 20 h with $D_2O$ in a humid atmosphere. (b) $^{1}$H MAS-NMR spectra of samples (i) hydrated, (ii) dried at 60 °C, (iii) rehydrated 2 h 30 min, and (iv) rehydrated 20 h with $D_2O$.

linewidths of components at −8 and −22/−30 ppm are considerably lower than those of the parent sample, suggesting that the amount of both types of sodium have been reduced during the exchange. Quantitative analysis of the $^{23}$Na spectrum of this sample shows that the structural formula can be expressed now as $(Na_{0.08})_s(Na_{0.46})_pH_{0.46}NbWO_6$. Thus, Na ions are preferentially exchanged in square channels; however, the formation of this phase requires that a large amount of Na ions also be exchanged in pentagonal channels. In particular, Na ions responsible for the shoulder at −22/−30 ppm have been completely eliminated in the exchanged sample.

To analyze OH groups created during exchanging processes, we have also recorded $^{23}$Na MAS-NMR spectra with the CP (cross polarization) technique. In general, it is observed, in agreement with previous works, that contact times required for the magnetization transfer from protons to quadrupole nuclei are very short. In the analyzed compound, the maximum transfer of polarization to B and C signals was obtained for contact times near 350 $\mu$s. This observation suggests, in agreement with quantitative determinations carried out in $^{23}$Na MAS-NMR spectra, that the Na/H distribution is similar, and proton exchange has been produced in both square and pentagonal channels.

$^{1}$H MAS-NMR spectra of the exchanged sample $Na_{0.54}H_{0.46}NbWO_6$ are formed by two components at ca. 2 and 6.5 ppm that have been ascribed to OH groups (Figure 7b). The comparative analysis of the parent and exchanged samples shows that the narrow band at 5 ppm, ascribed to adsorbed water, is not detected here. This is in agreement with TGA data because hydration water was not detected in the $Na_{0.54}H_{0.46}NbWO_6$ sample. On the contrary, intensities of bands ascribed to OH groups, which were also detected in the parent sample, have increased considerably as a consequence of exchange reactions (compare vertical display scales of Figures 4 and 7b).

**Table 1.** Summary of the Quantitative Analysis of $^{23}$Na MAS-NMR Spectra of Dried $Na_{1-x}H_xNbWO_6$ Samples[a]

| H $x$ | Na $1-x$ | Na s | Na p | Na p/s |
|---|---|---|---|---|
| 0 | 1 | 0.19 | 0.81 | ∼4 |
| 0.32 | 0.68 | 0.14 | 0.54 | ∼4 |
| 0.46 | 0.54 | 0.08 | 0.46 | ∼6 |

[a] The amount of sodium ions in the square (s) and pentagonal (p) channels is indicated as well as the $(Na)_p/(Na)_s$ ratio.

Additional information has been extracted from the intermediate-exchanged sample $Na_{0.68}H_{0.32}NbWO_6 \cdot 0.1H_2O$. The analysis of TGA results previously reported[9] indicated the presence of adsorbed water, hydration water, and two types of OH groups. $^{23}$Na MAS-NMR spectra of as-prepared and hydrated samples are similar, indicating that hydratable $Na^+$ ions located at pentagonal channels have already been exchanged by protons (Figure 8a, spectra (i), (ii), and (iii)). The deconvolution of these spectra again provided quadrupolar constants similar to those deduced for the two components in the parent sample. Quantitative analysis of the spectrum of the sample dried at 60 °C (spectrum (iii)) showed that structural formula of this compound can be expressed as $(Na_{0.14})_s(Na_{0.54})_pH_{0.32}NbWO_6$. In this case, the hydration of the dried sample does not appreciably affect the $^{23}$Na MAS-NMR spectrum of this sample.

A summary of the chemical compositions and results of the quantitative analysis of NMR spectra for both parent and exchanged dried samples is shown in Table 1. It can be observed that in the formation of the derivatives, a large amount of sodium is exchanged in square and pentagonal channels. However, the $(Na)_p/(Na)_s$ ratio obtained for the sample with the highest exchange rate indicates that vacancies are preferentially created at the square channels.

The $^{1}$H MAS-NMR spectra of hydrated and dried $Na_{0.68}H_{0.32}NbWO_6$ samples are shown in Figure 8b. The $^{1}$H MAS-NMR spectrum of the partially hydrated TTB-like

spectrum (i) exhibits the presence of a single band arising from hydration water; however, when the sample is heated to 60 °C, adsorbed water is lost and two bands ascribed to OH groups are detected at ca. 2 and 6.5 ppm (spectrum (ii)). The observation of a single, narrow component in the hydrated sample at 6 ppm can be explained by assuming the existence of exchange processes between the protons of water molecules and OH groups. In this case, proton dipolar interactions are strongly reduced by the mobility of water. The elimination of water allows the detection of two broad NMR components, ascribed to OH groups, in which dipolar interactions between neighboring protons considerably enlarge the linewidth of the components.

It is interesting to remark that the better resolution of the two components at 2 and 6.5 ppm in $^1$H MAS-NMR spectra of samples rehydrated in a $D_2O$ atmosphere (Figures 4b and 8b) is a consequence of the reduction of H−H dipolar interactions produced by exchange processes between OH groups and $D_2O$ molecules. In this case, the increase of OD groups considerably reduces dipolar interactions (the nuclear magnetic moment of deuterons is 6 times lower than that of protons). However, the detection of separated components at 2, 5, and 6.5 ppm indicates that exchange processes between OH and water molecules are slow at room temperature. This explains the low values of conductivity measured at room temperature in exchanged dried samples. Conductivity increases 3 orders of magnitude in the hydrated sample when the temperature is increased to 90° in the presence of a water-saturated atmosphere. These experiments point to the proton as the charge carrier in conductive processes, rather than the remaining sodium ions.

## Conclusions

Preparation of $NaNbWO_6$, with the TTB structure, by the ceramic procedure has proven to be feasible. Electron Diffraction (ED) revealed the coexistence of two closely related TTB-like phases with similar cell parameters. One of them adopts the ideal TTB structure, whereas the other displays a monoclinic distortion of this structure. The composition and morphology of the two phases are similar, although the monoclinic phase is shown to be slightly tungsten deficient with respect to the nominal composition. $^{23}$Na MAS-NMR spectra of $NaNbWO_6$ have been interpreted on the basis of the ideal structure of TTB. Two signals were ascribed to Na ions located in channels with square and pentagonal sections (−8 and −22/−30 ppm, respectively). From the relative intensities of both signals in the spectra of dried samples, the distribution of sodium ions in two channels was deduced; according to this, the structural formula $(Na_{0.81})_p(Na_{0.19})_sNbWO_6$ has been deduced. $^1$H MAS-NMR spectra of hydrated samples has shown that a hydrolysis reaction occurs in the presence of atmospheric water.

The exchange of protons increases considerably in derivatives prepared by reaction with a stronger acid, $HNO_3$ (aq). The average structure and the morphology remain unchanged in $Na_{1-x}H_xNbWO_6$ derivatives. $^1$H and $^{23}$Na MAS-NMR spectroscopy has been used to monitor changes produced during exchange processes. It has been shown that the exchange of Na ions is mainly produced (but not exclusively) at square channels. The partial occupation of structural sites by sodium deduced from $^{23}$Na NMR spectra in the most-exchanged product is $\sim(Na_{0.46})_p(Na_{0.08})_sH_{0.46}NbWO_6$. However, a large amount of Na ions at the pentagonal channels do not exchange with protons, suggesting that these ions are needed to stabilize the bronze-like structure.

The rehydration of analyzed samples with deuterated water considerably improved the experimental resolution. This fact favored the detection of two types of OH groups in partially hydrated samples. The detection of a band at 5 ppm indicates that deuterons of adsorbed water exchange with the protons of OH groups in the sample; however, proton−deuteron exchange processes are slow at room temperature. This observation explains the low values of conductivity measured at room temperature and the activation of proton conductivity at increasing temperatures. The strong increase on conductivity, observed at 90 °C under a humid atmosphere, is now explained, and $H^+$ ions are signaled as charge carriers. As reported in other conducting materials, the presence of water seems to considerably improve proton conductivity.

**Acknowledgment.** This work has been financially supported by the MEC (Grant MAT2004-03070-C05) and the Comunidad de Madrid (Grant S-0505/PPQ/0358). The authors thank Universidad San Pablo-CEU for financial and continuous support.

IC0701312